Nuclear Medicine and Biology 41 (2014) 856–862

Contents lists available at ScienceDirect

Nuclear Medicine and Biology

journal homepage: www.elsevier.com/locate/nucmedbio

Diversity of RGD radiotracers in monitoring antiangiogenesis of flavopiridol and paclitaxel in ovarian cancer xenograft-bearing mice

Guangjie Yang [a], Hukui Sun [b], Yu Kong [a], Guihua Hou [b,*], Jiankui Han [a,**]

[a] Department of Nuclear Medicine, Qilu Hospital, Shandong University, Jinan, China
[b] Biomedical Isotope Research Center, School of Medicine, Shandong University, Jinan, China

ARTICLE INFO

Article history:
Received 29 May 2014
Received in revised form 4 August 2014
Accepted 5 August 2014

Keywords:
^{99m}Tc
RGD peptide
Mechanism
Ovarian cancer
Monitoring antiangiogenesis therapy
Integrin αvβ3

ABSTRACT

Introduction: Although encouraging results had been shown in antiangiogenesis therapy monitoring, the underlying mechanism of RGD radiotracer accumulation needs to be further illustrated. This study was aimed to investigate the diversity of RGD radiotracers in monitoring antiangiogenic agent's effects and the underlying mechanism in ovarian cancer-bearing mice with a new agent flavopiridol compared with paclitaxel.

Methods: Ovarian cancer SKOV-3 xenograft-bearing mice were established and divided into three groups, flavopiridol, paclitaxel and control. Flavopiridol (5 mg/kg body weight) and paclitaxel (20 mg/kg body weight) were administered every 3 days for 16 days. Tumor growth and proliferation were monitored by caliper measurements and immunofluorescence staining. Antiangiogenic effects were determined by tumor microvessel density (MVD) in vivo and by endothelial cell tube formation assay in vitro, respectively. ^{99m}Tc-3P-RGD$_2$ was prepared, and its biodistribution studies were carried out. The effect of antiangiogenesis therapy on integrin αvβ3 expression was studied by immunohistochemical staining and flow cytometry.

Results: Both paclitaxel and flavopiridol therapy could apparently inhibit tumor growth and proliferation, and antiangiogenic effects of therapy were validated in vivo and in vitro. However, compared with the control group, ID%/g tumor uptake of ^{99m}Tc-3P-RGD$_2$ showed a significant decrease at 2 hours (by 39.96% ± 8.23%, P = 0.044) and at 4 hours (by 35.76% ± 11.42%, P = 0.024) post injection in the paclitaxel-treated group, but a slight increase of tumor uptake in the flavopiridol-treated group at 2 hours (by 4.42% ± 0.24%, p = 0.898) and at 4 hours (by 12.2% ± 1.84%, P = 0.702). The further studies indicated flavopiridol therapy has a dual-effect, reducing integrin αvβ3 expression on endothelial cells due to the reduction of tumor MVD and up-regulating the integrin αvβ3 expression on tumor cells.

Conclusions: There is diversity in evaluating antiangiogenic response when using ^{99m}Tc-3P-RGD$_2$, which may be an important reminder in future clinical applications of RGD radiotracers as a strategy for antiangiogenesis therapy response monitoring.

1. Introduction

Molecular imaging for noninvasive assessment of angiogenesis represents potential interest for clinicians since antiangiogenic drugs have been successfully used in cancer patients. One promising approach is to identify molecular markers of angiogenesis by conjugating a specific ligand recognizing overexpressed receptors in angiogenic tumors to imaging probes [1]. In this area, one of the most potential and best studied targets is the integrin αvβ3 [2], which is probably the most strongly involved in the regulation of tumor angiogenesis among all integrins [1]. Integrin αvβ3 is expressed on tumor neovessels as well as on some tumor cells but not on quiescent blood vessels in normal tissue [3,4]. Due to the high integrin αvβ3 binding affinity, many RGD peptides probes have been developed for multimodality imaging of integrin expression with the purpose of tumor diagnosis and tumor treatment response monitoring [5–10].

There have been several studies using suitably labeled RGD peptides tracers to monitor chemotherapy or antiangiogenesis therapy efficacy. Paclitaxel, ZD4190 (a small-molecular-weight VEGF receptor-2 tyrosine kinase inhibitor), Dasatinib and Abraxane were employed for different types of tumors including lung cancer, breast carcinoma and glioblastoma in previous studies [11–15], and all the above researches concluded that RGD radiotracers had a good ability in noninvasive monitoring antiangiogenic response in the solid tumors. However, in preliminary experiment we found that flavopiridol, a "special" antiangiogenic agent, CDK (cyclin-dependent kinase) inhibitor, can additionally up-regulate the integrin αvβ3 expression on tumor cells, while inhibiting tumor angiogenesis in ovarian cancer animal models. The dual-effect of antiangiogenic drugs may affect the ability to evaluate antiangiogenic response when using RGD radiotracers.

* Correspondence to: G. Hou, PhD, MD, Biomedical Isotope Research Center, School of Medicine, Shandong University, No. 44 Wenhuaxi Road, Jinan 250012, China. Tel./fax: +86 531 88382096.
** Correspondence to: J. Han, MD, Department of Nuclear Medicine, Qilu Hospital, Shandong University, No. 107 Wenhuaxi Road, Jinan 250012, China. Tel./fax: +86 531 82169661.
E-mail addresses: ghhou1@hotmail.com (G. Hou), hanjiank@163.com (J. Han).

http://dx.doi.org/10.1016/j.nucmedbio.2014.08.008
0969-8051/

In this study, two antiangiogenic drugs, flavopiridol and paclitaxel were selected to check if there exists diversity of RGD radiotracers in monitoring antiangiogenic therapy to different antitumor agents and its molecular mechanism.

2. Materials and methods

2.1. Preparation of ^{99m}Tc-3P-RGD$_2$

^{99m}Tc-3P-RGD$_2$ denotes [^{99m}Tc(HYNIC-3PRGD$_2$)(tricine)(TPPTS)] (HYNIC = 6-hydrazinonicotinyl; TPPTS = trisodium triphenylphosphine-3,3′,3′′-trisulfonate; 3PRGD$_2$ = PEG$_4$-E[PEG$_4$-c(RGDfK)]$_2$; and PEG$_4$ = 15-amino-4,7,10,13-tetraoxapentadecanoic acid). ^{99m}Tc-3P-RGD$_2$ was prepared by a lyophilized kit formulation [16] kindly provided by Shuang Liu in School of Health Sciences of Purdue University. The kit was formulated by containing per mL, 20 μg of HYNIC-3PRGD$_2$, 5 mg of TPPTS, 6.5 mg of tricine, 40 mg of mannitol, 38.5 mg of disodium succinate hexahydrate, and 12.7 mg of succinic acid.

For ^{99m}Tc radiolabeling, the kit vials were brought to room temperature immediately before use. To the kit vial was added 1 mL of Na^{99m}TcO4 solution (1110–1850 MBq) in saline. After brief vortexing, the vial was heated at 100 °C for 20 min. After radiolabeling, the vial was allowed to stand at room temperature for 5 min. A sample of the resulting solution was analyzed by radio instant thin layer chromatography (ITLC) and analytical radio high performance liquid chromatography (HPLC). All the resulting solution was filtered with a 0.20-μm Millex-LG filter before being injected into animals.

For radio instant thin layer chromatography, a 1-μl sample of the resulting solution was spotted on a chromatography paper (Whatman no. 1) and developed in acetone as the mobile phase. For HPLC, HPLC was done in C-18 reverse phase column (4.6 mm^3, 250 mm, 300 Å pore size). The mobile phase was isocratic with 90% solvent A (25 mM ammonium acetate buffer) and 10% solvent B (acetonitrile) at 0–2 min, followed by a gradient mobile phase going from 10% solvent B at 2 min to 15% solvent B at 5 min and 20% solvent B at 20 min.

2.2. Cell culture

The ovarian carcinoma cells SKOV-3 were purchased from ATCC (American Type Culture Collection, Manassas, VA) and cultured in McCoy's 5a Medium (Invitrogen, Carlsbad, CA), supplemented with 10% fetal bovine serum (Gibco BRL, Gaithersburg, MD). Human umbilical vein endothelial cells (HUVECs) were isolated from human umbilical cord veins by collagenase treatment as described previously [17]. HUVECs were cultured in ECM (endothelial cell growth media) medium (Clonetics Corp., San Diego, CA) supplemented with 10% fetal bovine serum. Cells were grown at 37 °C in an atmosphere of 5% CO_2.

2.3. Animal models

Female athymic nu/nu mice (Vital River Laboratories, Beijing, China) at 4–6 weeks of age were subcutaneously implanted with 5×10^6 SKOV-3 cells in 0.1 mL of saline into the left front flank. All procedures were performed in a laminar flow cabinet using aseptic techniques. The animals were allowed to feed ad libitum and used when the tumor volume reached about 50 mm^3 (8–10 days after implantation). Tumor growth was followed by caliper measurements of perpendicular diameters of the tumors. The tumor volume was estimated by the formula tumor volume = a * b * b/2, where a and b were the tumor′s greatest diameter and smallest diameter, respectively, in millimeters.

2.4. Paclitaxel and flavopiridol therapy protocol

We utilized ovarian carcinoma mouse model to evaluate the ability of ^{99m}Tc-3P-RGD$_2$ in monitoring the therapeutic response of paclitaxel (Sigma-Aldrich, St. Louis, MO, USA) and flavopiridol (Selleck Chemicals, Houston, TX, USA). Paclitaxel and flavopiridol were dissolved in dimethylsulfoxide and diluted by PBS to specified concentrations before use. The final concentration of dimethylsulfoxide in treated cultures was <0.1%. For biodistribution studies, 24 mice with ovarian cancer were divided into 3 groups by means of random number table (n = 8/group). The mice were treated according to one of the following conditions. Briefly, the mice were injected i.p. with 0.1 ml of flavopiridol at a dosage of 5 mg/kg body weight (flavopiridol-treated group), with 0.1 ml of paclitaxel at a dosage of 20 mg/kg body weight (paclitaxel-treated group), and with 0.1 ml of PBS (control group). Therapies were performed every 3 days for 16 days (6 injections), and the day when the first injection of drugs was performed was considered day 0.

2.5. Biodistribution protocol

SKOV-3 xenograft-bearing mice were injected with 0.37 MBq/0.1 ml (10 μCi/0.1 ml) ^{99m}Tc-3P-RGD$_2$ via tail vein to evaluate the biodistribution of the tracer in the major organs and tumor of mice. Four mice were sacrificed at 2 and 4 hours post injection in each group. Blood, tumor, major organs and tissues were collected, weighed, and counted using a γ counter. The results were presented as percentage of injected dose per gram of tissue (%ID/g). For the blocking experiment, E[c(RGDfK)]$_2$ (custom-made by ChinaPeptides Co., Ltd., Shanghai, China) was dissolved in the solution containing ^{99m}Tc-3P-RGD$_2$ to give a concentration of 3.5 mg/ml (excess, ~14 mg/kg). Four SKOV-3 xenograft-bearing mice were used and each animal was injected with 0.1 ml of the above solution containing 0.37 MBq ^{99m}Tc-3P-RGD$_2$ along with E[c(RGDfK)]$_2$. All four animals were sacrificed at 2 hours post injection for organ biodistribution using the same procedure above.

2.6. Endothelial cell tube formation assay

Twenty-four-well plates were coated with 100 μL of Matrigel (Becton Dickinson, Bedford, MA) and polymerized for 30 min at 37 °C. HUVECs were pretreated by flavopiridol (300 nM) or paclitaxel (100 nM) at 37 °C for 24 h before being plated at a concentration of 3×10^4 cells/well in 500 μL of ECM medium supplemented with 2% fetal bovine serum onto the layer of Matrigel. Subsequently, five random fields of each well were digitally photographed to analyze tube formation. Quantification of endothelial cell tube formation is by counting the number of tube-like structures from three independent tube formation experiments [18].

2.7. Tumor tissue immunohistochemistry and detection of MVD

Immunohistochemical analysis of the xenografted tumor tissues harvested from the 12 mice was performed one day after the biodistribution studies at 4 hours post injection. Briefly, after rehydration, 4-μm sections of paraffin-embedded tissue on glass slides were incubated in 3% hydrogen peroxide to block the endogenous peroxidase activity. After trypsinization, sections were blocked by incubation in 3% bovine serum albumin in PBS. Sections were incubated with primary antibodies against CD34, Ki-67 and integrin αv (anti both human and mouse integrin αv, Abcam Inc., Cambridge, MA, USA) overnight at 4 °C. The addition of secondary antibodies and color development followed the manufacturer's instructions. Photographs were acquired and then quantified by Image-Pro Plus. For each sample, all available fields (up to five random fields), visualized under a ×40 objective lens, were used for measurements.

MVD was evaluated by immunohistochemical analysis with antibodies to the endothelial marker CD34 and determined according to the method of Weidner [19]. Briefly, the immunostained sections were initially screened at low magnification (×40) to identify hot spots, which are the areas of highest neovascularization. Any yellow brown-stained endothelial cell or endothelial cell cluster that was clearly separate from adjacent microvessels, tumor cells and other

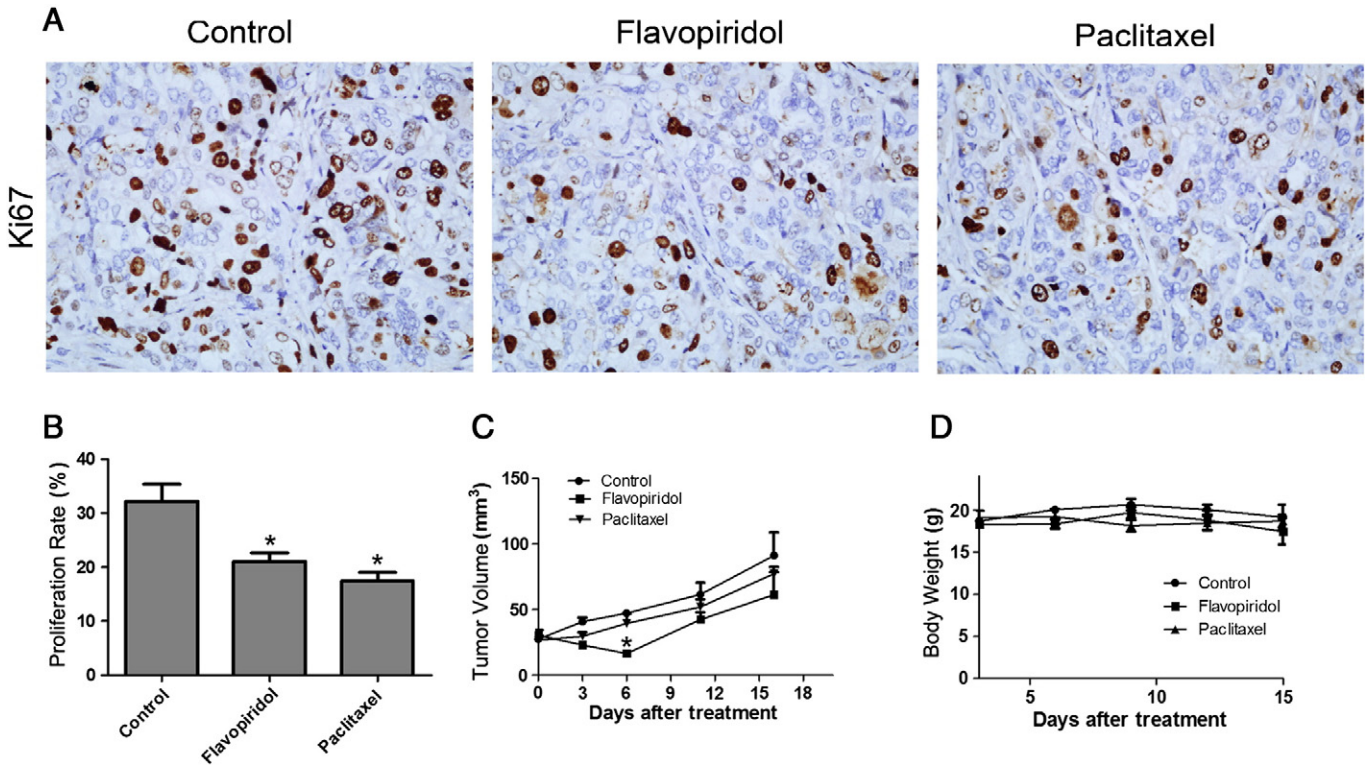

Fig. 1. Effects of paclitaxel and flavopiridol therapy on tumor proliferation and growth in SKOV-3 xenografts. A. Representative Ki-67 staining of SKOV-3 xenografts from animals in the three groups (images at 40× magnification). B. Comparison of proliferation rates from quantitative evaluation of Ki-67 staining. *P < 0.05 versus control group. C. Summary of primary tumor volumes of animals in the three groups in the SKOV-3 models. Tumor volumes were determined by caliper measurements. *P < 0.05 versus control group. D. Body weight changes of animals in the three groups.

connective tissue elements was considered a single, countable microvessel. Within the hot spot area, the stained microvessels were counted in a single high-power field (×200), and the average vessel count in 5 hot spots was considered the value of MVD.

2.8. Flow cytometric analysis

This study sought to determine the response of integrin αvβ3 expression on SKOV-3 cells to the pretreatment with paclitaxel and flavopiridol. Briefly, cells growing in monolayer culture at 60%–80% confluence were washed with PBS and detached with trypsin at 37 °C after the 24 h pretreatment with 300 nM flavopiridol or 100 nM paclitaxel. Then cells were fixed for 10 min in 4% paraformaldehyde at ambient temperature. Subsequently, cells were constituted to 5×10^6 cells/mL, and 200 μL was incubated with FITC-conjugated anti-αvβ3 antibody (eBioscience, San Diego, CA) and isotype control FITC-conjugated IgG at ambient temperature for 40 min. Cells were then washed again and analyzed by flow cytometry using FACS Calibur and CellQuest software.

2.9. Data analysis

Quantitative data were expressed as mean ± SD. Data were analyzed by t-test and chi-square test with GraphPad statistical software (GraphPad Software Inc., San Diego, CA, USA). Differences were considered significant at $P < 0.05$.

3. Results

3.1. Effects of paclitaxel and flavopiridol therapy on tumor growth and proliferation in SKOV-3 xenografts

Tumor volumes of SKOV-3 xenografts were monitored by caliper measurements every 3–5 days for the therapy period of 16 days with paclitaxel and flavopiridol (Fig. 1C). No significant difference was found in the initial tumor volumes between the groups. Tumors enlarged rapidly were observed in the control group, with a mean tumor volume doubling time of 3.95 ± 1.85 days. Repeated administration of paclitaxel or flavopiridol tended to slow the tumor growth. Compared with the control group, tumor sizes were slightly smaller in the paclitaxel-treated group. Reduction in tumor volume was more obvious in the flavopiridol-treated group. Especially, there was a significant reduction on day 6 in comparison with the control group ($P < 0.05$).

To further characterize tumor response to therapy, we investigated the degree of proliferation as assessed by Ki-67 immunohistochemical staining (Fig. 1A). There was a high percentage of Ki-67-positive cells (32.2% ± 7.5%) in the control group. Consistent with the therapy of paclitaxel and flavopiridol, tumor growth was inhibited, and delayed cell proliferation was observed in the paclitaxel-treated group (17.6% ± 3.6%) and in the flavopiridol-treated group (21.8% ± 5.1%) ($P < 0.05$) (Fig. 1B).

Paclitaxel or flavopiridol therapy seemed not to cause obvious side effects because no significant difference was observed in body weight between the paclitaxel or flavopiridol-treated and control mice (Fig. 1D), and no other signs of toxicity were noted.

3.2. Antiangiogenic effect of paclitaxel and flavopiridol in vitro and in vivo

To determine antiangiogenic effects of paclitaxel and flavopiridol in vivo, tumor angiogenesis was evaluated by CD34 immunohistochemical staining (Fig. 2A, upper panel). CD34 expression markedly decreased in the flavopiridol-treated group and the paclitaxel-treated group compared with the control group (by 77.7% ± 8.6% and 69.58% ± 6.7% respectively, both $P < 0.01$) (Fig. 2B). Similar to CD34 expression, flavopiridol and paclitaxel treatment led to a 65% and 56% reduction, respectively, in MVD levels (Fig. 2C).

The effects of paclitaxel and flavopiridol therapy on angiogenesis were also evaluated in vitro by endothelial cell tube formation assay

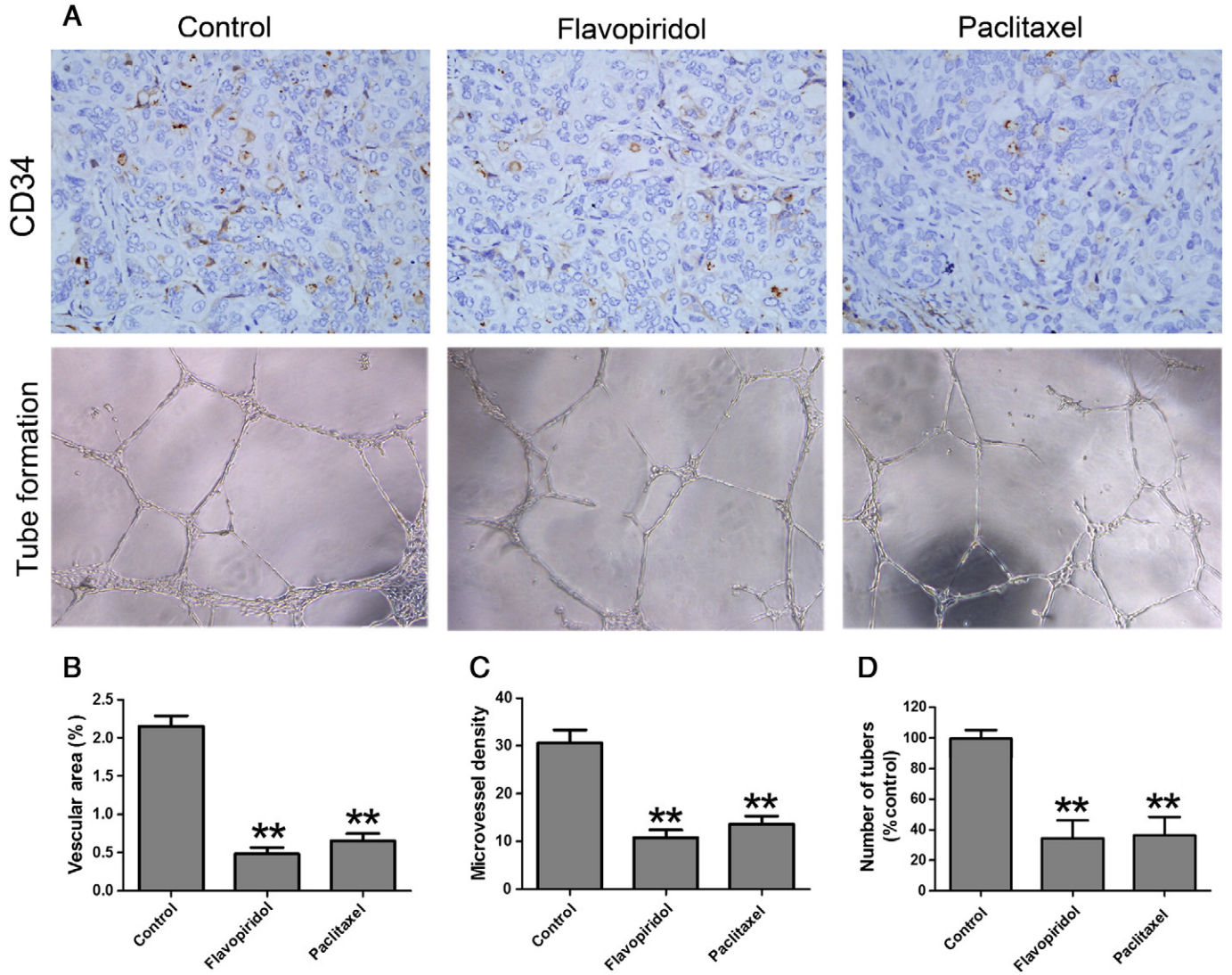

Fig. 2. Antiangiogenic effects of paclitaxel and flavopiridol in vivo and in vitro. A. Illustration of CD34 immunohistochemical detection in representative SKOV-3 xenografts (upper panel), and representative images of endothelial Matrigel tube formation in paclitaxel or flavopiridol-treated endothelial cells in comparison with untreated endothelial cells (lower panel). B. Quantitative analysis of the percentage of CD34 expression from animals in the three groups. C. Quantitative evaluation of microvessel density (MVD) by quantitating CD34-expressing vessels from hotspot areas, as described in Materials and methods. D. Quantification of endothelial cell tube formation by counting the number of tube-like structures from three independent tube formation experiments, $^{**}P < 0.01$ versus control group.

(Fig. 2A, lower panel), which is commonly used as an index of angiogenesis [20,21]. Compared with the formation of elongated and robust tube-like structures in the control group, paclitaxel and flavopiridol effectively abrogated the width and the length of endothelial tubes. The tube-forming network in the flavopiridol-treated group and the paclitaxel-treated group was drastically reduced compared with the control group (by 65.8% ± 7.4% and 63.8% ± 4.6%, respectively, both $P < 0.01$) (Fig. 2D).

Taken together, these results suggested that therapy with paclitaxel and flavopiridol could effectively inhibit tumor growth and angiogenesis in SKOV-3 xenografts.

3.3. Effects of paclitaxel and flavopiridol on ^{99m}Tc-3P-RGD$_2$ accumulation in SKOV-3 xenografts

The radiochemical purity of ^{99m}Tc-3PRGD$_2$ prepared from lyophilized kits determined by radio-ITLC was 97.86% ± 1.02% (Rf = 0, three times repeated) and by HPLC was 97.36% ± 0.87% (retention time = 9.8 min, three times repeated). The specific activity of ^{99m}Tc-3PRGD$_2$ was 185 GBq/μmol.

Biodistribution studies were performed to investigate the impact of paclitaxel and flavopiridol therapy on ^{99m}Tc-3P-RGD$_2$ accumulation in SKOV-3 xenografts. Data showed that ^{99m}Tc-3P-RGD$_2$, a new promising dimeric RGD radiotracer, exhibited rapid blood clearance and high kidney uptake (Fig. 3A).

In the paclitaxel-treated group, tumor uptake showed a significant decrease compared with the control group at 2 hours (by 39.96% ± 8.23%, P = 0.044) and at 4 hours (by 35.76% ± 11.42%, P = 0.024) after injection of ^{99m}Tc-3P-RGD$_2$ (Fig. 3B). The decrease of MVD may account for the reduction of ^{99m}Tc-3P-RGD$_2$ uptake in the paclitaxel-treated group. However, ^{99m}Tc-3P-RGD$_2$ had a different performance in the flavopiridol-treated group. There was no significant decrease but a slight increase of tumor uptake in the flavopiridol-treated group compared with the control group at 2 hours (by 4.42% ± 0.24%, P = 0.898) and at 4 hours (by 12.2% ± 1.84%, P = 0.702) post injection.

The blocking experiment was used to demonstrate the integrin αvβ3 specificity. Fig. 3 compares the selected organ uptake of ^{99m}Tc-3P-RGD$_2$ in the absence/presence of E[c(RGDfK)]$_2$ at 2 hours post injection. Co-injection of E[c(RGDfK)]$_2$ resulted almost complete

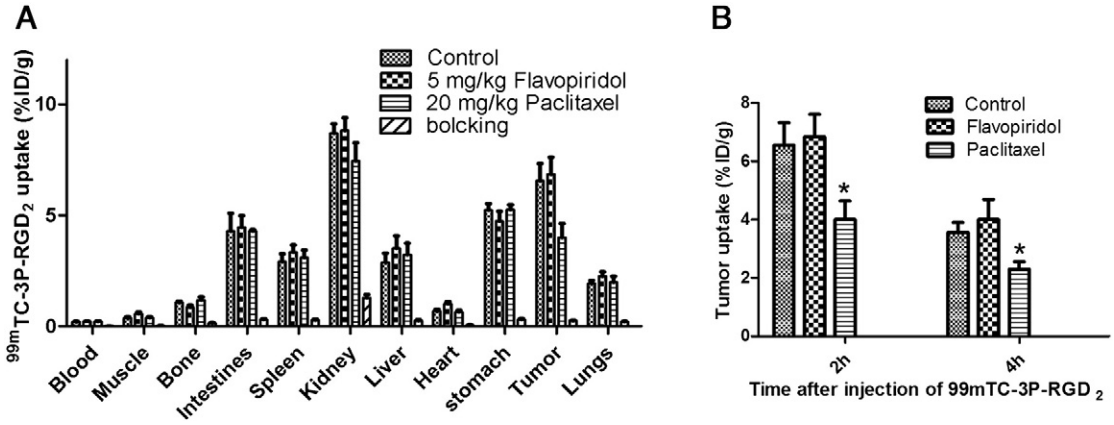

Fig. 3. Effects of paclitaxel and flavopiridol therapy on ^{99m}Tc-3P-RGD$_2$ accumulation in SKOV-3 xenografts. A. The quantified biodistribution of ^{99m}Tc-3P-RGD$_2$ at 2 hours post injection in the absence/presence of excess E[c(RGDfK)]$_2$ (350 μg/mouse) in the SKOV-3 xenograft-bearing mice. B. Comparison of changes in %ID/g tumor uptake of ^{99m}Tc-3P-RGD$_2$ after paclitaxel or flavopiridol therapy at 2 and 4 hours post injection. *P < 0.05 versus control group.

blockage of the tumor uptake for ^{99m}Tc-3P-RGD$_2$ (0.25 ± 0.03%ID/g with E[c(RGDfK)]$_2$ in blocking group vs. 6.56 ± 0.78%ID/g without E[c(RGDfK)]$_2$ in control group). There was also a significant reduction in radioactivity accumulation in non-cancerous organs, such as the heart, intestine, kidneys, lungs, liver, muscle and spleen.

These results indicate that RGD radiotracers may vary in the ability for therapeutic response monitoring to the therapy of antiangiogenic drugs in SKOV-3 models.

3.4. Effects of paclitaxel and flavopiridol therapy on integrin expression in SKOV-3 xenografts and tumor angiogenesis in vivo and in vitro

The uptake of ^{99m}Tc-3P-RGD$_2$ was affected by the expression of integrin αvβ3 located on activated tumor vascular endothelial cells and on tumor cells. To investigate the mechanism of altered ^{99m}Tc-3P-RGD$_2$ uptake of SKOV-3 xenografts to different antiangiogenic drugs, integrin expression was evaluated by immunohistochemical staining, and correlated with the tumor uptake. Because integrin on tumor neovessels was of murine origin and that on tumor cells was of human origin, we stained tumor sections with both antimurine integrin αv and antihuman integrin αv antibodies. Compared with the control group, integrin αv expression was different in the paclitaxel-treated group and the flavopiridol-treated group (Fig. 4A and B). A significant decrease of αv expression was observed in the paclitaxel-treated group (by 34.2% ± 5.9%, P < 0.01), while a slight increase in the flavopiridol-treated group (by 8.7% ± 3.2%, P = 0.078). Correlation analysis showed that there was a linear correlation between the ^{99m}Tc-3P-RGD$_2$ tumor uptake and integrin αv expression (R = 0.785, Fig. 4C). The linear correlation indicated that ^{99m}Tc-3P-RGD$_2$ is reliable for specific imaging of integrin αvβ3 expression.

As described above, both paclitaxel and flavopiridol therapy decreased tumor MVD, but showed different effects on tumor uptake of ^{99m}Tc-3P-RGD$_2$. Therefore, we can speculate that there may be other pathway affecting on tumor uptake of RGD peptides. To study the further molecular mechanism, effects of paclitaxel and flavopiridol therapy on integrin αvβ3 expression on SKOV-3 cells were measured by flow cytometric analysis (Fig. 4D). Flavopiridol significantly increased integrin αvβ3 expression on SKOV-3 cells compared with that of untreated SKOV-3 cells(by 23.7% ± 5.1%, P < 0.05), while there was no significant difference in integrin αvβ3 expression between paclitaxel-treated SKOV-3 cells and untreated SKOV-3 cells.

These results demonstrate that tumor uptake of RGD radiotracer depends on the level of total integrin αvβ3 expression in the tumor, but the regulating effect of antiangiogenic drugs on integrin αvβ3 which was located on tumor cells might impair the reliability when ^{99m}Tc-3P-RGD$_2$ was used for evaluating the tumor angiogenesis.

4. Discussion

Flavopiridol is a semisynthetic flavonoid, which was originally isolated from the stem bark of the Indian plant *Dysoxylum binectariferum* [22]. The anticancer effect of flavopiridol has been identified by the National Cancer Institute (NCI) on 60 human cancer cell lines [23]. Flavopiridol has anticancer properties mainly due to its strong inhibiting activity for cdks (cyclin dependent kinases), and its cytotoxic activity of flavopiridol is not limited to cycling cells. Research in the last few years has indicated that besides inhibiting CDK activity, flavopiridol also possesses several important antiangiogenic activities including induction of apoptosis of endothelial cells [24]; inhibition of the hypoxic induction of VEGF and/or its production under hypoxic conditions through inhibition of HIF-1a transcription [25]; decreased secretion of MMPs that is linked with significant inhibition of invasive potential in Matrigel assays [26]. Paclitaxel, which is derived from the bark of the Pacific yew tree, is a promising anticancer drug shown to inhibit a wide variety of tumor cells, by diverse mechanisms that include cell cycle arrest, induction of apoptosis and stabilization of microtubules. In addition to this, inhibition of angiogenesis is an important supplement of its antitumor activity [27–29]. In the last decade, a number of studies showed that paclitaxel has antiangiogenic activity that could be ascribed to the inhibition of either tubule formation or cell migration [30]. We referred to administration regimens in other relevant studies [31,32] and a few modifications have been done according to the preliminary experiments. For flavopiridol, in fact, most of clinical studies are in combination regimes. In this study we focused on its antiangiogenesis activity and used in single-agent regime.

Many angiogenic inhibitors were used for antiangiogenesis therapy in various types of tumors in recent years. Despite the initial promising performance of angiogenic inhibitors in the clinic, how to monitor tumors responses to the therapy remains a major challenge [33]. Imaging of integrin αvβ3 expression may be a possible solution to the third problem. In the preclinical setting, a large variety of imaging strategies have been successfully employed for imaging of integrin expression, including PET or SPECT, MRI, targeted US and optical imaging [34]. Radionuclide techniques are advantageous owing to their high sensitivity, and up to now, the use of RGD radiotracers is still the only approach that has been successfully translated into the clinic [35].

Several labeled monomeric or dimeric RGD peptides tracers had been investigated to monitor antiangiogenesis therapy efficacy in recent

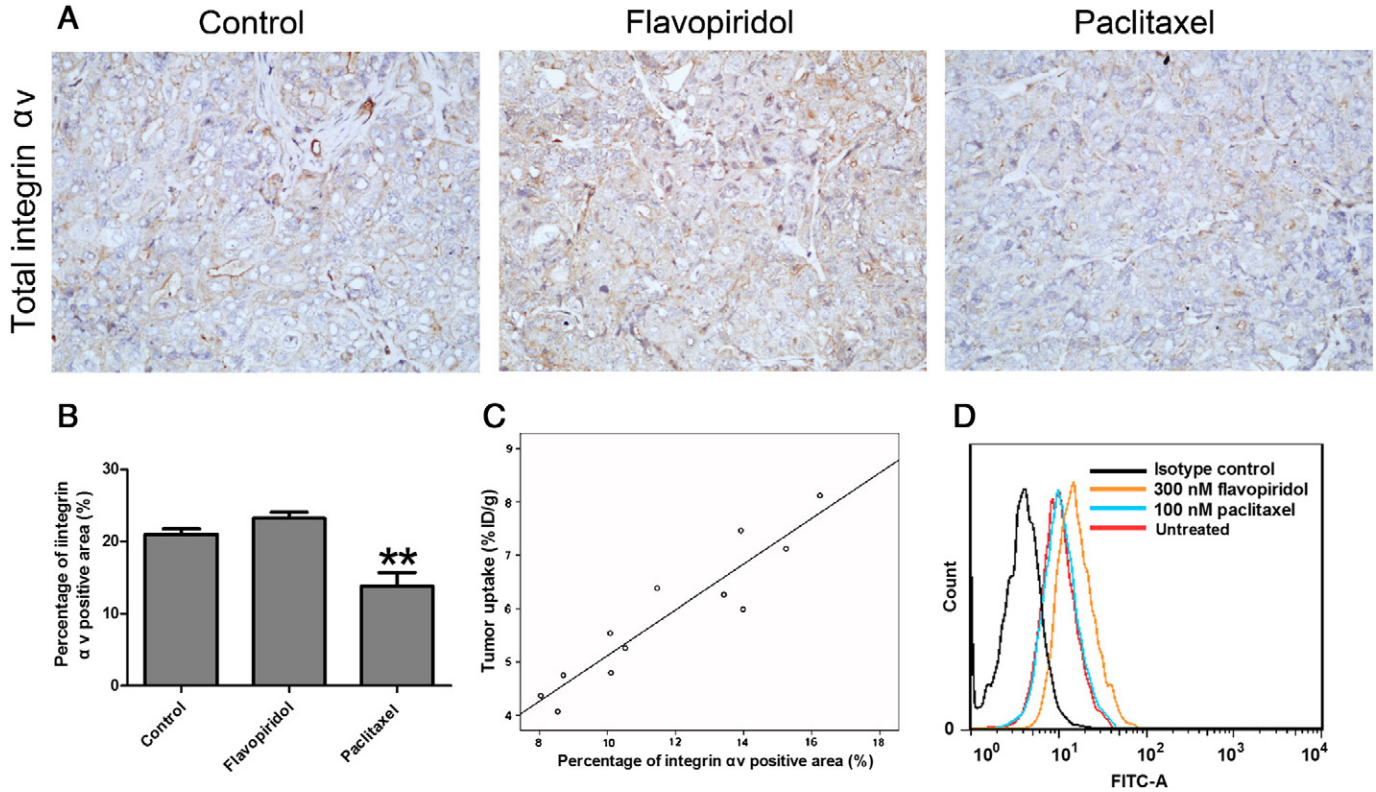

Fig. 4. Effects of paclitaxel and flavopiridol therapy on integrin expression on SKOV-3 xenografts and SKOV-3 cells. A. Representative integrin αv immunohistochemical staining of SKOV-3 xenografts from animals in the three groups (images at 40× magnification). For integrin αv antibodies used in the study were both of antimurine and of antihuman, the total integrin αv, including integrin αv on tumor (human origin) and on vessels (murine origin), was measured. B. Quantitative analysis of integrin αv expression from animals in the three groups. **P < 0.01 versus control group. C. Linear relationship between ^{99m}Tc-3P-RGD$_2$ accumulation and total integrin αv expression based on the %ID/g tumor uptake of ^{99m}Tc-3P-RGD$_2$ from the biodistribution studies and the total integrin αv expression from immunohistochemical staining. The data were obtained from 12 mice in all the three groups (4 mice per group) 4 hours after post injection of ^{99m}Tc-3P-RGD$_2$. D. Flow cytometry analysis of integrin αvβ3 expression in paclitaxel or flavopiridol-treated SKOV-3 cells in comparison with untreated SKOV-3 cells.

studies [13,14,36]. No clinical data regarding monitoring antiangiogenesis therapies are available on this subject yet, though some clinical trials have been completed [37,38] and the others are ongoing [39–41].

It is well established that integrin αvβ3 is highly expressed on the activated endothelial cells in newly formed blood vessels, thus representing an interesting molecular marker for angiogenesis imaging [42]. However, integrin αvβ3 is also expressed on some types of tumor cells. In this study, the linear correlation between the ^{99m}Tc-3P-RGD$_2$ tumor uptake and total integrin expression suggests RGD radiotracers are a reliable strategy for integrin αvβ3 expression, and which is consistent with the results from other preclinical and clinical studies [7,13,43]. So both parts of integrin αvβ3 can bind strongly to RGD peptides radiotracer. With the therapy of antiangiogenic drugs, the expression of integrin αvβ3 on tumor vascular endothelial cells decreases due to the decrease of tumor MVD. This is the general mechanism of RGD radiotracers in monitoring antiangiogenic effects. Additional regulating effect of antiangiogenic agents on the integrin αvβ3 on the tumor cells would have a negative influence when RGD peptide probes are used for monitoring.

Accordingly, distribution of integrin αvβ3 on tumor cells or activated endothelial cells has an important influence on the applications of RGD peptides probes imaging. How much of the contribution is from the tumor cells or the tumor neovessels depends largely on the tumor type [43,44]. Thus not all the cases with antiangiogenesis therapy are suitable for the response evaluation using RGD peptide radiotracer, especially when the antiangiogenic agents have an additional regulating effect on the integrin αvβ3 on the tumor cells. The most important issue is that altered uptake of RGD peptides radiotracer after antiangiogenesis therapy owing to the reduction of integrin αvβ3 on the tumor neovessels rather than on the tumor cells must be confirmed when RGD peptide radiotracer is used for antiangiogenesis therapy monitoring. Liu et al. [45] concluded that RGD peptide radiotracer would be a promising probe for characterizing tumor angiogenesis due to the good correlation between the probe uptake and the integrin αvβ3 expression on newborn blood vessels for patients with integrin αvβ3-negative tumors not for all the patients. It may be an insoluble situation when antiangiogenic agent regulates integrin αvβ3 expression on αvβ3-positive tumor cells, which will result in an unreliable evaluation of antiangiogenic response using RGD peptides radiotracers. In the present study, both the responses of antiangiogenesis therapy to paclitaxel and flavopiridol were confirmed in vivo and in vitro, but flavopiridol-treated animals had an “unmatched” uptake of RGD peptides radiotracer in comparison with paclitaxel-treated animals. The following studies of underlying mechanism indicate that flavopiridol therapy has a dual-effect on integrin αvβ3 expression on tumors, reducing integrin αvβ3 expression on endothelial cells due to the reduction of MVD and up-regulating the integrin αvβ3 expression on tumor cells.

4.1. Limitations

There are potential limitations to this study. First, the integrin αvβ3 on tumor cells and tumor newborn vasculature are of human origin and murine origin, respectively, in SKOV-3 xenograft models, while all the integrin αvβ3 are both of human origin in patients, but it is reported [45,46] that RGD peptide radiotracer would target both the integrin αvβ3 on tumor cells and tumor newborn vasculature in mouse tumor

models, which is the same as the clinical situation. Second, we detected integrin αv expression instead of integrin αvβ3, because there is no integrin αvβ3 antibody available for paraffin method, and integrin αv or integrin β3 expression was used for quantifying the expression of integrin αvβ3 in many previous studies [7,13,44].

In conclusion, the results indicated that there was diversity in evaluating antiangiogenic response when using RGD peptide radiotracer. The studies of mechanism suggested flavopiridol therapy has a dual-effect on the target of integrin αvβ3, thus leading to an unreliable evaluation of antiangiogenesis therapy response. The finding of this study may be an important reminder in future clinical applications of RGD radiotracers, and understanding the detailed mechanism of RGD peptide radiotracers imaging may aid the development of new monitoring strategies for selecting patient population and evaluating tumors responses to antiangiogenesis therapy.

References

[1] Danhier F, Le Breton A, Préat V. RGD-based strategies to target alpha(v) beta(3) integrin in cancer therapy and diagnosis. Mol Pharm 2012;9:2961–73.
[2] Beer AJ, Schwaiger M. Imaging of integrin alphavbeta3 expression. Cancer Metastasis Rev 2008;27:631–44.
[3] Brooks PC, Montgomery AM, Rosenfeld M, Reisfeld RA, Hu T, Klier G, et al. Integrin alpha v beta 3 antagonists promote tumor regression by inducing apoptosis of angiogenic blood vessels. Cell 1994;79:1157–64.
[4] Weis SM, Lindquist JN, Barnes LA, Lutu-Fuga KM, Cui J, Wood MR, et al. Cooperation between VEGF and beta3 integrin during cardiac vascular development. Blood 2007;109:1962–70.
[5] Moncelet D, Bouchaud V, Mellet P, Ribot E, Miraux S, Franconi JM, et al. Cellular density effect on RGD ligand internalization in glioblastoma for MRI application. PLoS One 2013;8:e82777.
[6] Metz S, Ganter C, Lorenzen S, van Marwick S, Herrmann K, Lordick F, et al. Phenotyping of tumor biology in patients by multimodality multiparametric imaging: relationship of microcirculation, alphavbeta3 expression, and glucose metabolism. J Nucl Med 2010;51:1691–8.
[7] Haubner R, Weber WA, Beer AJ, Vabuliene E, Reim D, Sarbia M, et al. Noninvasive visualization of the activated alphavbeta3 integrin in cancer patients by positron emission tomography and [18F]Galacto-RGD. PLoS Med 2005;2:e70.
[8] Chen WT, Shih TT, Chen RC, Tu SY, Hsieh WY, Yang PC. Integrin αvβ3-targeted dynamic contrast-enhanced magnetic resonance imaging using a gadolinium-loaded polyethylene gycol-dendrimer-cyclic RGD conjugate to evaluate tumor angiogenesis and to assess early antiangiogenic treatment response in a mouse xenograft tumor model. Mol Imaging 2012;11:286–300.
[9] Guo N, Lang L, Li W, Kiesewetter DO, Gao H, Niu G, et al. Quantitative analysis and comparison study of [18F]AlF-NOTA-PRGD2, [18F]FPPRGD2 and [68Ga]Ga-NOTA-PRGD2 using a reference tissue model. PLoS One 2012;7:e37506.
[10] Sirsi SR, Flexman ML, Vlachos F, Huang J, Hernandez SL, Kim HK, et al. Contrast ultrasound imaging for identification of early responder tumor models to anti-angiogenic therapy. Ultrasound Med Biol 2012;38:1019–29.
[11] Sun X, Yan Y, Liu S, Cao Q, Yang M, Neamati N, et al. 18F-FPPRGD2 and 18F-FDG PET of response to Abraxane therapy. J Nucl Med 2011;52:140–6.
[12] Yang M, Gao H, Yan Y, Sun X, Chen K, Quan Q, et al. PET imaging of early response to the tyrosine kinase inhibitor ZD4190. Eur J Nucl Med Mol Imaging 2011;38:1237–47.
[13] Jung KH, Lee KH, Paik JY, Ko BH, Bae JS, Lee BC, et al. Favorable biokinetic and tumor-targeting properties of 99mTc-labeled glucosamino RGD and effect of paclitaxel therapy. J Nucl Med 2006;47:2000–7.
[14] Dumont RA, Hildebrandt I, Su H, Haubner R, Reischl G, Czernin JG, et al. Noninvasive imaging of alphaVbeta3 function as a predictor of the antimigratory and antiproliferative effects of dasatinib. Cancer Res 2009;69:3173–9.
[15] Ji S, Zheng Y, Shao G, Zhou Y, Liu S. Integrin α(v)β3-targeted radiotracer (99m)Tc-3P-RGD2 useful for noninvasive monitoring of breast tumor response to antiangiogenic linifanib therapy but not anti-integrin α(v)β3 RGD2 therapy. Theranostics 2013;3:816–30.
[16] Jia B, Liu Z, Zhu Z, Shi J, Jin X, Zhao H, et al. Blood clearance kinetics, biodistribution, and radiation dosimetry of a kit-formulated integrin αvβ3-selective radiotracer 99mTc-3PRGD2 in non-human primates. Mol Imaging Biol 2011;13:730–6.
[17] Masuyama J, Berman JS, Cruikshank WW, Morimoto C, Center DM. Evidence for recent as well as long term activation of T cells migrating through endothelial cell monolayers in vitro. J Immunol 1992;148:1367–74.
[18] Wani AA, Jafarnejad SM, Zhou J, Li G. Integrin-linked kinase regulates melanoma angiogenesis by activating NF-κB/interleukin-6 signaling pathway. Oncogene 2011;30:2778–88.
[19] Weidner N, Semple JP, Welch WR, Folkman J. Tumor angiogenesis and metastasis: correlation in invasive breast carcinoma. N Engl J Med 1991;324:1–8.
[20] Auerbach R, Lewis R, Shinners B, Kubai L, Akhtar N. Angiogenesis assays: a critical overview. Clin Chem 2003;49:32–40.
[21] Jin BY, Sartoretto JL, Gladyshev VN, Michel T. Endothelial nitric oxide synthase negatively regulates hydrogen peroxide-stimulated AMP-activated protein kinase in endothelial cells. PNAS 2009;106:17343–8.
[22] Takada Y, Aggarwal BB. Flavopiridol inhibits NF-kappaB activation induced by various carcinogens and inflammatory agents through inhibition of IkappaBalpha kinase and p65 phosphorylation: abrogation of cyclin D1, cyclooxygenase-2, and matrix metalloprotease-9. J Biol Chem 2004;279:4750–9.
[23] Kelland LR. Flavopiridol, the first cyclin-dependent kinase inhibitor to enter the clinic: current status. Expert Opin Investig Drugs 2000;9:2903–11.
[24] Brusselbach S, Nettlebeck DM, Sedlacek HH, Muller R. Cell cycle-independent induction of apoptosis by the anti-tumor drug flavopiridol in endothelial cells. Int J Cancer 1998;77:146–52.
[25] Melillo G, Sausville EA, Cloud K, Lahusen T, Varesio L, Senderowicz AM. Flavopiridol, a protein kinase inhibitor, down-regulates hypoxic induction of vascular endothelial growth factor expression in human monocytes. Cancer Res 1999;59:5433–7.
[26] Li Y, Bhuiyan M, Alhasan S, Senderowicz AM, Sarkar FH. Induction of apoptosis and inhibition of c-erbB-2 in breast cancer cells by flavopiridol. Clin Cancer Res 2000;5:223–9.
[27] Lau DH, Xue L, Young LJ, Burke PA, Cheung AT. Paclitaxel (Taxol): an inhibitor of angiogenesis in a highly vascularized transgenic breast cancer. Cancer Biother Radiopharm 1999;14:31–6.
[28] Merchan JR, Jayaram DR, Supko JG, He X, Bubley GJ, Sukhatme VP. Increased endothelial uptake of paclitaxel as a potential mechanism for its antiangiogenic effects: potentiation by Cox-2 inhibition. Int J Cancer 2005;113:490–8.
[29] Pasquier E, Carre M, Pourroy B, Camoin L, Rebai O, Briand C, et al. Antiangiogenic activity of paclitaxel is associated with its cytostatic effect, mediated by the initiation but not completion of a mitochondrial apoptotic signaling pathway. Mol Cancer Ther 2004;3:1301–10.
[30] Bocci G, Di Paolo A, Danesi R. The pharmacological bases of the antiangiogenic activity of paclitaxel. Angiogenesis 2013;16:481–92.
[31] Reiner T, de las Pozas A, Perez-Stable C. Sequential combinations of flavopiridol and docetaxel inhibit prostate tumors, induce apoptosis, and decrease angiogenesis in the Ggamma/T-15 transgenic mouse model of prostate cancer. Prostate 2006;66:1487–97.
[32] Belotti D, Vergani V, Drudis T, Borsotti P, Pitelli MR, Viale G, et al. The microtubule-affecting drug paclitaxel has antiangiogenic activity. Clin Cancer Res 1996;2:1843–9.
[33] Shojaei F. Anti-angiogenesis therapy in cancer: current challenges and future perspectives. Cancer Lett 2012;320:130–7.
[34] Cai W, Chen X. Multimodality molecular imaging of tumor angiogenesis. J Nucl Med 2008;49:S113–28.
[35] Gaertner FC, Kessler H, Wester HJ, Schwaiger M, Beer AJ. RGD radiotracers for imaging and therapy. Eur J Nucl Med Mol Imaging 2012;39:S126–38.
[36] Jin ZH, Furukawa T, Claron M, Boturyn D, Coll JL, Fukumura T, et al. Positron emission tomography imaging of tumor angiogenesis and monitoring of antiangiogenic efficacy using the novel tetrameric peptide probe 64Cu-cyclam-RAFT-c(-RGDfK-)4. Angiogenesis 2012;15:569–80.
[37] Edward Aten. Edward Aten. Efficacy study of [F-18]RGD-K5 positron emission tomography (PET) as a tool to monitor response to an anti-angiogenic drug (K5-101); 2009 [ClinicalTrials.gov].
[38] Jeffrey Winick. A Proof-of-concept study to assess the ability of [18F]AH-111585 PET imaging to detect tumours and angiogenesis; 2007 [ClinicalTrials.gov].
[39] Woo Kyung Moon. PET-MR for prediction and monitoring of response to neoadjuvant chemotherapy in breast cancer; 2010 [ClinicalTrials.gov].
[40] Fergus Gleeson. RGD-PET-CT in cancer angiogenesis; 2011 [ClinicalTrials.gov].
[41] Gambhir Sanjiv. 18F FPPRGD2 positron emission tomography/computed tomography in predicting early response in patients with cancer receiving anti-angiogenesis therapy; 2013 [ClinicalTrials.gov].
[42] Zhou Y, Chakraborty S, Liu S. Radiolabeled cyclic RGD peptides as radiotracers for imaging tumors and thrombosis by SPECT. Theranostics 2011;1:58–82.
[43] Zhou Y, Kim YS, Chakraborty S, Shi J, Gao H, Liu S. 99mTc-labeled cyclic RGD peptides for noninvasive monitoring of tumor integrin αVβ3 expression. Mol Imaging 2011;10:386–97.
[44] Horton MA. The αvβ3 integrin "vitronectin receptor". Int J Biochem Cell Biol 1997;29:721–5.
[45] Liu Z, Jia B, Shi J, Jin X, Zhao H, Li F, et al. Tumor uptake of the rgd dimeric probe (99m)Tc-G3-2P4-RGD2 is correlated with integrin αvβ3 expressed on both tumor cells and neovasculature. Bioconjug Chem 2010;21:548–55.
[46] Liu Z, Liu S, Niu G, Wang F, Liu S, Chen X. Optical imaging of integrin αVβ3 expression with near-infrared fluorescent RGD dimer with tetra(ethylene glycol) linkers. Mol Imaging 2010;9:21–9.